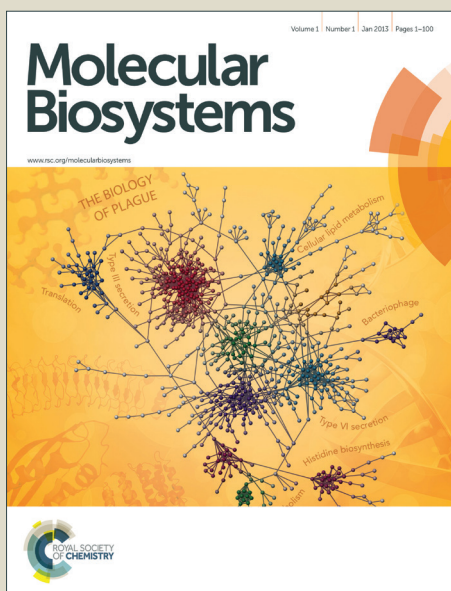


Molecular BioSystems

Accepted Manuscript



This is an *Accepted Manuscript*, which has been through the Royal Society of Chemistry peer review process and has been accepted for publication.

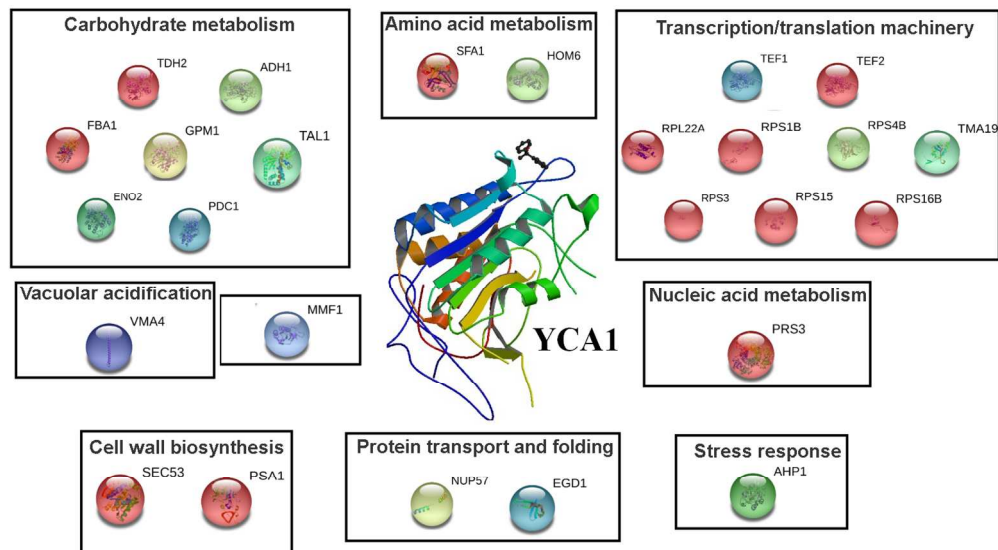
Accepted Manuscripts are published online shortly after acceptance, before technical editing, formatting and proof reading. Using this free service, authors can make their results available to the community, in citable form, before we publish the edited article. We will replace this *Accepted Manuscript* with the edited and formatted *Advance Article* as soon as it is available.

You can find more information about *Accepted Manuscripts* in the [Information for Authors](#).

Please note that technical editing may introduce minor changes to the text and/or graphics, which may alter content. The journal's standard [Terms & Conditions](#) and the [Ethical guidelines](#) still apply. In no event shall the Royal Society of Chemistry be held responsible for any errors or omissions in this *Accepted Manuscript* or any consequences arising from the use of any information it contains.



www.rsc.org/molecularbiosystems



Combined proteomic and metabolomic approach revealed new non-apoptotic roles of metacaspase YCA1 gene in *Saccharomyces cerevisiae*, highlighting its involvement in the cell metabolism and stress response. 563x319mm (72 x 72 DPI)

Differential proteome-metabolome profiling of *YCA1*-knock-out and wild type cells reveals novel metabolic pathways and cellular processes dependent on the yeast metacaspase.

Maša Ždravčić^{**a}, Valentina Longo^{*b}, Nicoletta Guaragnella^a, Sergio Giannattasio^a, Anna Maria Timperio^{#b} and Lello Zolla^{#b}

The yeast *Saccharomyces cerevisiae* expresses one member of metacaspase Cys protease family, encoded by *YCA1* gene. Combination of proteomics and metabolomics data showed *YCA1* deletion down-regulated glycolysis, TCA cycle and alcoholic fermentation as compared with WT cells. $\Delta yca1$ cells also showed a down-regulation of the pentose phosphate pathway and an accumulation of pyruvate, correlated with higher levels of certain amino acids found in these cells. Accordingly, there is a decrease in protein biosynthesis, and up-regulation of specific stress response protein like Ahp1p, which possibly provides these cells with a better protection against stress. Moreover, in agreement with the down-regulation of protein biosynthesis machinery in $\Delta yca1$ cells, we have found that regulation of transcription, co-translational protein folding and protein targeting to different subcellular locations were also down-regulated.

Metabolomics analysis of the nucleotide content showed a significant reduction in $\Delta yca1$ cells in comparison with the WT, except for GTP content which remained unchanged. Thus, our combined proteome/metabolome approach added a new dimension to the non-apoptotic function of yeast metacaspase, which can specifically affect cell metabolism through as yet unknown mechanisms and possibly stress-response pathways, like HOG and cell wall integrity pathways. Certainly, *YCA1* deletion may induce compensatory changes in stress response proteins offering a better protection against apoptosis to $\Delta yca1$ cells rather than a loss in a pro-apoptotic *YCA1*-associated activity.

1. Introduction

Mammalian caspases are the best studied of a large family of multifunctional proteases sharing a common caspase-haemoglobinase fold (CHF) ¹. Caspases have a cysteine-dependent aspartate-specific protease activity with a central role in apoptosis, the major form of programmed cell death (PCD), and inflammation²⁻⁴. Proper regulation of apoptosis is critical for both development and tissue homeostasis, and malfunction of apoptosis contributes to the development of human diseases⁵⁻⁷. Caspase-mediated cleavage of specific substrates is responsible for most of the visible changes that characterize apoptotic cell death ⁸. Caspases are synthesized as catalytically inactive zymogens that can be activated by a proteolytic cleavage by a processing caspase, or by holoenzyme formation ^{3, 9}. Paracaspases, found in animals and slime molds, and metacaspases, from plants, fungi and protozoa, are two other classes of multifunctional CHF proteases, phylogenetically related to mammalian caspases ^{1, 10} whose biochemistry and function are still poorly characterized (for refs see ¹¹).

The discovery that the yeast *Saccharomyces cerevisiae* can undergo a form of PCD sharing several morphological and biochemical features with mammalian apoptosis ¹² has further confirmed this unicellular eukaryote as an ideal model to study the molecular pathways regulating cell stress response and PCD ^{13, 14}. With this respect, it is of note that *S. cerevisiae* expresses a single metacaspase encoded by *YCA1* gene. Yca1p undergoes caspase-like autocatalytic activation, similar to mammalian caspases ¹⁵. *YCA1* was first implicated in PCD regulation in yeast: its overexpression coupled with oxidative stress or prolonged culture triggers cell death while its deletion decreases H₂O₂- or age-induced PCD ¹⁵. However, metacaspase-dependent and -independent PCD pathways have been shown in yeast ¹⁶. Interestingly, although *YCA1* can modulate somehow a z-VAD-fmk-inhibited caspase-like activity ^{15, 17}, its protein product lacks Asp specificity and cleaves its targets preferentially after Arg or Lys residues (for refs see ¹¹).

Recent investigations have also revealed a number of non-apoptotic cellular processes in which *YCA1* is involved. *YCA1* is implicated in cell cycle control; its deletion or catalytic inactivation was shown to alter cell cycle dynamics ¹⁸. In addition, *YCA1* contributes to the fitness and adaptability of growing yeast through clearance of insoluble protein aggregates in an Hsp104 disaggregase and proteasome-dependent manner¹⁹⁻²¹. Finally, *YCA1* was reported to be implicated in the regulation of antioxidant status and mitochondrial respiration^{22, 23}. Yet, both Yca1p biochemistry and physiological function in yeast are still elusive.

For the past decade, considerable effort has been invested in maturing proteomic technology to deliver information at a rate and cost commensurate to transcriptomic technologies. Proteomics technologies offer considerable opportunities for improved biological understanding and biomarker discovery. The central platform for proteomics is tandem mass

spectrometry (MS) but a number of other technologies, resources, and expertise are absolutely required to perform meaningful experiments. The combination of complementary approaches on the protein and on the peptide level provided an almost complete overview of the proteome of entire cell like yeast or organelles by countervailing mutual drawbacks. Yates and co-workers reported the first large-scale yeast proteome study in 2001 with the identification of 1483 proteins following ≈ 68 h of mass spectral analysis, i.e. 0.4 proteins were identified per minute²⁴. Relative proteomic changes induced by *YCA1* ablation in BY4741 background identified proteins involved in vacuolar catabolism, stress response, mitochondria-associated factors, the 20S proteasome and DNA repair proteins as species unique to *YCA1*-knock-out ($\Delta yca1$) strain^{18,19}. In addition, a proteomic approach was used to understand the role of Yca1 in protein aggregate formation and dissolution²⁰. Nevertheless, the only specific substrate of yeast metacaspase identified to date is the enzyme glyceraldehyde-3-phosphate dehydrogenase (GAPDH)²⁵.

For a better understanding of physiological role of *YCA1* in yeast cell, we combine proteomic and metabolomic data in order to provide valuable insight into conditional changes in the metabolic activity. While transcriptomics and proteomics provide important insights into the hierarchical regulation of metabolic flux, metabolomics shed light on the actual enzyme activity through metabolic regulation and mass action effects. Metabolomics is a comprehensive tool for monitoring processes within biological systems²⁶. In fact, in a systemic viewpoint relevant biological information on living systems can be grasped from the study of small, albeit pivotal molecules, which constitute the fundamental bricks of metabolic pathways. Thus, proteomics and metabolomics offer a nonbiased suite of tools to address physiologic mechanisms from various levels by integrating signal transduction, cellular metabolism, and phenotype analysis.

In this context to better understand the physiological role of *YCA1* in yeast cell, the total cellular proteomic analysis of wild type and $\Delta yca1$ yeast cell was performed. By combining proteomics and metabolomics techniques, we linked alterations of protein expression to metabolism. Technical aspects of rapid-resolution reversed-phase HPLC on-line with mass spectrometry are hereby described. Finally, our results revealed that *YCA1* is crucial in regulation of carbohydrate, amino acid and nucleotide metabolism and confirmed that its deletion causes a general decrease in protein synthesis and transport with an increase in cell stress response.

2. Results and Discussion

2.1 Differential proteomic and metabolomic analysis of WT and $\Delta yca1$ W303-1B cells

In order to get an insight into the function of yeast metacaspase gene *YCA1* the effect of its deletion on protein abundance was analyzed by comparative proteomic and metabolomic analysis between WT and knock-out W303-1B strain growing in mid-exponential phase. The total cellular proteomes of WT and $\Delta yca1$ cells were obtained by 2-DE, and a total of 23 spots with altered amount of proteins in $\Delta yca1$ cells (5 with increased and 18 with decreased amount) were successfully identified by using mass spectrometry analysis (Fig. 1). To maximize performance we used a cellular lysis approach, employed trypsin digestion, and used dimethyl sulfoxide (DMSO, 5%) as an LC additive to increase abundance of acidic peptides and unify charge state in agreement to^{26,27}. In our case DMSO improved performance, as reported by Herbert et al.²⁸, thus we included it in all subsequent experiments. MS analysis showed that these spots corresponded to 26 proteins, which were classified into functional groups (Table 1 Supplementary material). Several cellular processes were altered in the *YCA1*-lacking strain, including: i) metabolism of carbohydrates, ii) amino acids and iii) nucleotides, iv) transcription/translation machinery, v) protein transport and folding, vi) stress response, vii) cell wall biosynthesis and viii) vacuolar acidification. Relative expression changes of proteins altered in $\Delta yca1$ cells are represented in Fig 2. The number and the corresponding name(s) of the identified proteins are indicated for each spot. Spots 753, 474, 1031, 1029, 1939, 1926 and 1949 (corresponding to Tdh2, Prs3, Tef 1/2, Rps3 and Nup57) were detected only in wild type cells, whereas two spots 773 and 570 (corresponding to Ahp1 and Vma/Sec54) were present only in $\Delta yca1$ cells. The details of triplicate 2-D gel images of these spots are shown in Fig. 3.

Our results, using W303-1B strain, significantly differ qualitatively and quantitatively from the $\Delta yca1$ cell proteomic profile characterized in BY4741 yeast strain: 59 and 13 proteins were found in higher and lower amounts, respectively, in *YCA1*-knock-out BY4741 cells¹⁹. This is mainly due to differences in both strains and growth conditions analysed in the two studies. Although W303-1B and BY4741 cells were grown in glucose rich medium, in the case of BY4741 cells the growth medium pH has been set to 3.5 with HCl. Thus, the $\Delta yca1$ W303-1B proteome profile obtained in this study is the first analysed at normal growth conditions (pH \sim 6.8). In fact, although there is no significant difference in the growth rate of either strains between normal and low pH growth medium, the acid environment used in the BY4741 study changed the pattern of gene expression observed at normal pH, causing metabolic re-programming and cellular adaptation^{29,30}.

Furthermore, to characterize the role of *YCA1* in yeast cell metabolism, we have performed HPLC-MS analysis of selected metabolites related to metabolic pathways altered by *YCA1* deletion. Our metabolomics approach allows to discriminate and quantify a wide array of metabolites with extreme specificity and sensitivity, thus enabling to perform complex investigations

even on extremely low quantities of biological material. The advantages also include the possibility to perform targeted investigations on a single (or a handful of) metabolite(s) simultaneously through single (multiple) reaction monitoring, which further improves the dynamic range of concentrations to be monitored. Files have been processed through MAVEN, an open-source software program for interactive processing of LC-MS-based metabolomics data. MAVEN enables rapid and reliable metabolite quantisation from multiple reaction monitoring data or high-resolution full-scan mass spectrometry data. It automatically detects and reports peak intensities for isotope-labelled metabolites³¹. Metabolite assignment was further elaborated in the light of the hydrophobicity/hydrophilicity of the compound and its relative retention time in the RP-HILIC-HPLC run. Quantification of metabolites from carbohydrate, amino acid and nucleic acid metabolism and cell wall biosynthesis is shown in Fig. 4.

In the next sections an integration of metabolomics and proteomics results, with special attention to those most affected metabolisms, will be discussed separately from the other cellular processes found to be affected by *YCA1* deletion.

2.2 *ΔYCA1* cells have altered carbohydrate, amino acid and nucleotide metabolism

2.2.1 Carbohydrate metabolism

Glucose is the preferred carbon and energy source for yeast cells, but also an important primary messenger molecule, responsible for the down-regulation of respiration, gluconeogenesis and metabolism of other sugars³². In the exponential phase of growth, *S.cerevisiae* cells metabolize glucose mostly by fermentation to ethanol, despite the presence of oxygen³³. We have found decreased amounts of all the seven proteins involved in carbohydrate metabolism in *Δyca1* cells. Fructose 1,6-bisphosphate aldolase (Fba1p), glyceraldehyde-3-phosphate dehydrogenase (Tdh2p/GAPDH), glycerate phosphomutase (Gpm1p) and enolase II (Eno2p) are glycolytic/gluconeogenic enzymes; pyruvate decarboxylase (Pdc1p) and alcohol dehydrogenase (Adh1p) are involved in alcohol fermentation; and finally transaldolase (Tal1p) is a protein of pentose phosphate shunt.

GAPDH, already shown to be a specific target of metacaspase upon H₂O₂-induced apoptosis in yeast²⁵, was detected within two spots; 753 and 882, with significantly different MW both representing protein fragments. Silva et al. showed by digestome analysis that GAPDH fragmentation is a biological phenomenon that occurs also independently on metacaspase activity, but additional protein fragments were detected under stressed-induced active metacaspase conditions²⁵. As shown in Fig. 3, we detected spot 753 exclusively in WT cells, so this higher level of GAPDH fragmentation in WT cells is in agreement with the finding that specific GAPDH cleavage products occur only when metacaspase is active, that is in WT cells. Moreover, we performed bioinformatics analysis by analyzing GAPDH protein sequence for the presence of metacaspase-specific tripeptide cleavage sites with paired basic amino acid residues at P1 and P2 positions³⁴, and identified the presence of Arg-specific cleavage site (GGR) at position 198 (Table 1). This is in agreement with first indications that GAPDH contains endopeptidase target-sequences distinct from the ones recognized by mammalian caspases²⁵. Yet, further biochemical and functional studies in physiological conditions are needed to identify the actual metacaspase-specific cleavage site(s) in GAPDH. As a whole, these results confirm the validity of our experimental approach for exploring *YCA1* function in yeast. We thus extended the bioinformatics analysis to all other differentially expressed proteins identified in our analysis as for the presence of putative metacaspase-specific cleavage sites. Seven proteins, beyond GAPDH were identified containing a metaspase-specific cleavage site and are reported in Table 1. Each protein identified will be discussed in the next sections with the relevant cellular process in which it is involved.

Metabolomics analysis showed that the intracellular concentrations of glycolytic intermediates were significantly lower (about 56%) in *Δyca1* with respect to WT cells (Fig. 4), which is consistent with the decreased amount of glycolytic enzymes determined by proteomic analysis. Thus, *Δyca1* cells showed decreased glycolysis with respect to the WT cells. The amount of tricarboxylic (TCA) acid cycle intermediates, citrate, malate and fumarate, also decreased in *Δyca1* cells, suggesting a down-regulation of respiratory activity, as already reported²³. Interestingly, pyruvate levels were found to be higher in *Δyca1* than in WT cells. This accumulation of pyruvate could be at least partially explained by decreased levels of the two enzymes of alcoholic fermentation, Pdc1p) and Adh1p, required for the reduction of acetaldehyde to ethanol. Finally, Adh1p was identified as a putative *YCA1* substrate (Table 1), and it was detected in two spots (972 and 349) with different isoelectric points that could represent possible protein isoforms.

We have also found that Tal1p level decreased in *Δyca1* cells. Tal1p is a cytosolic transaldolase that converts sedoheptulose 7-phosphate and glyceraldehyde 3-phosphate to erythrose 4-phosphate and fructose 6-phosphate, important for the non-oxidative branch of the pentose phosphate pathway (PPP). Consistent with the lower amount of Tal1p found in these cells, erythrose 4-phosphate and D-ribose 5-phosphate had lower concentrations in *Δyca1* cells (Fig.4). By sharing some

intermediate metabolites with glycolysis, Tal1p act as a bridge between glycolysis and PPP.

Altogether, these results showed a down-regulation of central carbon metabolism in *Δyca1* cells, including glycolysis, alcoholic fermentation and PPP with significant pyruvate accumulation. This in part could account for increased amount of amino acids induced by *YCA1* deletion (see below).

2.2.2 Amino acid metabolism

Sfa1p, a bifunctional enzyme, containing both alcohol dehydrogenase and glutathione-dependent formaldehyde dehydrogenase activities, was found in lower amount in *Δyca1* cells. It is involved in the Ehrlich pathway for valine, isoleucine, phenylalanine, leucine and tryptophan degradation³⁵, as well as in detoxification of formaldehyde³⁶. In fact, the concentrations of valine, leucine, isoleucine, phenylalanine and tryptophane were significantly higher in *Δyca1* than in the WT cells (Fig. 4). Accordingly, Pdc1p and Adh1p, two other enzymes involved in Ehrlich pathway³⁷, were down-regulated (see section 2.2.1). These results are also in agreement with the high levels of pyruvate observed in *Δyca1* cells, since pyruvate is a precursor of valine, leucine and isoleucine. Transcription of *SFA1* is controlled by the HOG pathway, which controls cell response to osmotic shock³⁸. In response to hyperosmotic stress yeast cells undergo PCD in a *YCA1*-dependent manner as shown by reduced cell death in *Δyca1*³⁹. Thus, whether and how *YCA1* is related to HOG pathway deserves further investigation. It is of note that, differently from other aromatic amino acids, histidine levels were lower (37%) in *Δyca1* with respect to the WT cells.

Another enzyme of amino acid metabolism was found in lower amount to be down-regulated in the cells lacking *YCA1* (Fig. 2). The first enzyme is homoserine dehydrogenase (Hom6p), which catalyzes the third step in the common pathway for methionine and threonine biosynthesis from aspartate⁴⁰. Metabolomics analysis revealed that L-threonine concentration was lower in *Δyca1* with respect to WT cells, which is in agreement with proteomics data, while L-methionine concentration remains virtually unchanged (Fig. 4).

2.2.3 Nucleotide metabolism

Beyond the relative proteomic changes identified in carbohydrate and amino acid metabolism, only one enzyme, 5-phosphoribosyl-1(α)-pyrophosphate synthetase (Prs3p), involved into nucleotide metabolism, was detected exclusively in WT cells (Fig. 3). Prs3p catalyzes biosynthesis of phosphoribosyl pyrophosphate (PRPP). PRPP is an important biosynthetic intermediate, a precursor for the production of purine, pyrimidine, and pyridine nucleotides and the amino acids histidine and tryptophan, and is required for both *de novo* and the salvage pathways of nucleotide metabolism⁴¹. Accordingly, metabolomics analysis of the *Δyca1* cells showed a significant reduction in nucleotide content as compared with that of the WT cells, except for GTP content which remained virtually unchanged. Indeed, adenine nucleotides (AMP+ADP) were ~54% of the WT levels, GMP 60% of the WT levels and uridine nucleotides (UMP+UDP) 40% of the WT levels (Fig. 4), consistent with the down-regulation of Prs3p. The absence of Prs3p in *YCA1*-knock-out cells could also in part explain the decreased histidine content observed in these cells (see section 2.2.2). The apparent decrease in nucleotide content in *Δyca1* cells complies with a longer G1/S transition accompanied by slower growth of these cells in fermentation conditions¹⁸.

Interestingly, Prs3p harbours a metacaspase-specific cleavage site (Table 1). We could speculate that *YCA1* may have a role in Prs3p maturation, with Prs3p precursor protein being more susceptible to degradation in *Δyca1* cells, in which the protein is not detected.

2.3 Protein biosynthesis, transport and folding are down-regulated in cells lacking *YCA1*

The amount of eight proteins involved in protein biosynthesis and ribosome biogenesis was found to be altered in *Δyca1* cells. These proteins mainly showed a lower level (88%) than that in WT cells. Translation elongation factor (Tef1/2p) was detected in five different spots in WT cells. Spots 1031, 1029, 1939 and 1949 represent protein isoforms, whereas spot 1926 has a lower Mr and represent a putative protein fragment (Fig. 1). However, none of the five spots was detected in *Δyca1* cells, as shown in Fig. 3. Six ribosomal proteins were found to decrease their expression in *Δyca1* cells (Table 1 Supplementary material). Ribosomal protein of the small (40S) subunit (Rps3p) was identified in three spots, two of which could represent protein isoforms (1031 and 1949) and spot 649 might represent a fragmented form. Spots 1031 and 1949 are detected exclusively in WT cells (Fig. 3). Another ribosomal protein, Rps4b, was identified in two spots, that differed only by their pI, suggesting a possible additional PTM (Fig. 1). In both Rps3p and Rps4b ribosomal subunits we have identified the presence of Arg-specific putative cleavage sites (Table 1). Thus, we could speculate that *YCA1* is somehow involved in

maturation of functional Rps4bp and Rps3p.

In agreement with the decreased level of proteins involved in the translation machinery observed in *Δyca1* cells, we have found decreased amount of proteins regulating co-translational protein folding and protein targeting to different subcellular locations. Two proteins (Egd1p and Nup57p) involved in protein transport and folding were found to be down-regulated in cells lacking *YCA1*. Egd1p is a subunit of the nascent polypeptide-associated complex (NAC), involved in regulation of 'de novo' co-translational protein folding, post-translational protein targeting to membrane and unfolded protein binding. NAC complex is associated with cytoplasmic ribosomes and has a role in protein targeting to many subcellular locations, including mitochondria⁴². Nup57p is an essential component of the central core of nuclear pore complex (NPC), responsible for the nucleocytoplasmic transport of macromolecules. Nup57p is one of the proteins identified as a potential *YCA1* substrate (Table 1).

Altogether, these results suggest a lower efficiency of protein synthesis machinery in *Δyca1* cells, according to Shrestha et al.,²⁰ that confirm a major role of *YCA1* in cell stress response. Indeed, since *YCA1* has a major role in proteostasis *Δyca1* cells may use a compensatory mechanism to limit protein production during stress²⁰. Ribosome biogenesis is energetically expensive to the cell; it utilizes ~90 % of the total cellular energy of exponentially growing yeast cells⁴³. Thus, down-regulation of the translation machinery is in agreement with the overall decrease in central carbon metabolism found in *Δyca1* cells.

Within this class of proteins, Tma19p (Mmi1p) is the only protein found to be accumulated in *Δyca1* cells. Tma19p is the yeast orthologue of mammalian translationally-controlled tumor protein (TCTP), which has presumably anti-apoptotic functions in humans and interacts with translational machinery⁴⁴. It has been shown that induction of apoptosis in *S. cerevisiae* cells by oxidative stress, replicative ageing or mutation of *cdc48* leads to translocation of Mmi1p from the cytoplasm to the mitochondria, and it also interacts with microtubules, stabilizing them⁴⁴. The functional significance of Mmi1p transfer to mitochondria upon stress is still not clear, but the comparison with the mammalian system could offer an explanation of this transfer serving an anti-apoptotic function. Co-regulation of TCTP with ribosomal proteins has already been indicated by bioinformatics and experimental data⁴⁴. Also, cells lacking *MMI1* showed increased resistance to oxidative stress, as in *YCA1*-lacking cells^{22,44}, but how *MMI1* and *YCA1* are interrelated deserves further investigations.

2.4 *Δyca1* cells are in oxidizing condition

Genetic ablation of *YCA1* caused accumulation of alkyl hydroperoxide reductase (Ahp1p), a thiol-specific peroxiredoxin, involved in cellular response to oxidative stress. Ahp1p was identified in *Δyca1* cells in two different spots with the same Mr, but slightly different pI, suggesting additional post-translational modification (PTM). Actually, one of the Ahp1p isoforms (spot 773) was detected exclusively in *Δyca1* cells (Fig. 3). In fairly good agreement with our data, transcription of most of the genes involved in antioxidant defence mechanisms was shown to be repressed in *Δyca1* cells, except for an increase in *AHP1* transcription²³. This result indicates a shift in *Δyca1* cell redox balance towards more oxidizing conditions. Although exponentially growing *Δyca1* cells have essentially unchanged ROS levels compared to WT cells^{18,45}, these cells have been shown to have increased total and oxidized (GSSG) glutathione content in comparison with WT cells²³. *YCA1* has already been implicated in the regulation of antioxidant defences; *YCA1* deletion leads to a large H₂O₂-dependent accumulation of intracellular oxidized proteins and a compensatory increase in 20S proteasome activity, an essential part of the protein oxidation surveillance mechanism²².

In addition, increased expression of molecular chaperones and activation of stress response pathways in *Δyca1* yeast cells has been already shown, in a different genetic background and environmental conditions¹⁹. Those and our data further support the hypothesis that *Δyca1* cells may be pre-conditioned to sudden insults. *YCA1* deletion may induce compensatory changes in stress response proteins offering a better protection against apoptotic insults to *Δyca1* cells^{17,19}, rather than a loss in a pro-apoptotic *YCA1*-associated activity (for Ref. see⁴⁶).

2.5 Cell wall biosynthesis is altered in *Δyca1* cells

The expression of two enzymes involved in the cell wall biosynthesis, phosphomannomutase (Sec53p) and GDP-mannose pyrophosphorylase (Psa1p), was found to be altered by *YCA1* deletion. Sec53p was present exclusively in *Δyca1* cells (Fig. 3). It is involved in synthesis of GDP-mannose and dolichol-phosphate-mannose and required for folding and glycosylation of secretory proteins in the ER lumen, as well as in protein targeting to ER. Sec53p catalyzes the conversion of mannose-6-phosphate to mannose-1-phosphate, an intermediate in the cell wall biosynthesis⁴⁷. Psa1p, an enzyme catalyzing the next step in the pathway, the synthesis of GDP-mannose from mannose-1-phosphate and GTP, was found to be down-regulated in *Δyca1* cells. Psa1p was identified as a putative *YCA1* substrate (Table 1). However, our metabolic analysis showed a 50% increase in the concentration of GDP-mannose in *Δyca1* cells (Fig. 4), accordingly with Sec53p up-regulation. The yeast cell wall has diverse physiological functions: it maintains cell shape and integrity, and protects cell interior from environmental

stresses. Proteins glycosylated by long chains of mannose residues represent 40-50 % of the cell wall mass⁴⁸. Thus, an increase in GDP-mannose levels in *Δyca1* cells could influence the capacity of dynamical remodelling of the cell wall upon environmental stresses (see section 2.4).

2.6 Other cellular processes affected by *YCA1* deletion

Accumulation of other stress-related proteins has been observed in *Δyca1* cells. Subunit E of the V1 domain of the vacuolar H⁺-ATP-ase (Vma4p) was found exclusively in *Δyca1* cells (Fig. 3). Vacuolar ATP-ases are ATP-dependent proton pumps with a role in acidifying vacuolar compartments, which provides the driving force for secondary transport of variety of ions and metabolites⁴⁹. *Δyca1* BY4741 cells grown in low pH medium were shown to be enriched in vacuolar peptidases and to accumulate autophagic bodies, implying that a limited autophagic process occurs in these cells¹⁹. In this study, *Δyca1* W303-1B cells are viable cells at normal pH, with the growth rate comparable to that of WT cells, and it has also been shown that basal macroautophagy levels in exponentially growing WT and *Δyca1* cells are essentially the same⁵⁰. Thus, *YCA1* may have a role in intracellular pH homeostasis.

HRR25-interacting protein (Hri1p), whose function is unknown, showed increased amount in *Δyca1* cells. The function of Hri1p is still not completely understood, but in fission yeast Hri1p is known to function as a kinase of initiation factor 2 α (eIF2 α), involved in the regulation of protein synthesis in response to various environmental stresses. Hri1p was shown to be activated by both nitrogen starvation and stationary phase entry stresses⁵¹. Hri1p is the only protein accumulated in *Δyca1* cells harboring a putative metacaspase cleavage site (Table 1), suggesting that Hri1p may be degraded by *YCA1*.

Finally, the amount of mitochondrial protein Mmf1p, involved in maintenance of mitochondrial genome⁵², was found to decrease in cells lacking *YCA1*. Mmf1p is also required for transamination of isoleucine but not of valine or leucine and may regulate specificity of branched-chain transaminases Bat1p and Bat2p⁵³. Accordingly, an increase in isoleucine content was found in *Δyca1* cells (see section 2.2.2).

3. Materials and methods

3.1 Yeast strains, growth conditions and protein extraction

The *S. cerevisiae* strain used in this study were W303-1B (MAT α ade2 leu2 his3 trp1 ura3) (X.J. Chen's lab[§]) and *Δyca1* (W303-1B *yca1Δ::KanMX4*)¹⁷. Cells were streaked out freshly on a YPD plate from the -80 °C stock and incubated for two days at 30 °C. Cells were inoculated from starter cultures in YPD medium (1% yeast extract, 2% bactopectone, and 2% glucose) and grown at 26 °C with 150-rpm orbital rotation up to the mid-logarithmic phase (OD₆₀₀ = 0.7 – 0.8). For the extraction of proteins from yeast cells YPX™ Yeast Protein Extraction Kit (Expedeon) was used. Cells were harvested (5000 × g, at 4 °C for 5 min), and proteins were solubilized with extraction buffers provided in the kit, which contain SDS and reducing agents, providing unbiased extraction of proteins from cells. The buffers are designed to maximize the protein extraction and are compatible with downstream proteomics applications. Protease Inhibitor Cocktail (Sigma) was added to the cell lysate to improve the yield of intact proteins. The samples were denatured at 100 °C for 3 min, cooled down at 4 °C for 10 min, harvested at 20000 × g for 10 min to pellet the cellular debris and the supernatant was collected for the analysis. For accurate determination of total protein concentration, Bradford Ultra (Expedeon) assay, compatible with the presence of detergents was used.

3.2 2D-SDS-PAGE

For each sample, 600 μ g of proteins were precipitated for 90 min at 4 °C with a cold mix of tri-n-butyl phosphate/acetone/methanol (1:12:1) in ratio 1:4. This step is useful also to remove lipid component of the samples. After centrifugation, the pellets were solubilized in the buffer containing 7 M urea, 2 M thiourea, 4% (w/v) CHAPS, 40 mM Tris-HCl and were reduced and alkylated. Subsequently to a second precipitation, the samples were resuspended in rehydration solution (7M urea, 2M thiourea, 4% CHAPS and 1.25% v/v 3-10 carrier ampholyte (Bio-rad, CA, USA) and used to carry out passive rehydration of IPG strips (pH 3-10, non linear, 17 cm; Bio-Rad, CA, USA) over night. Isoelectrofocusing (IEF) was performed on an Protean IEF Cell (Bio-Rad, CA, USA) at 20 °C constant temperature and the total product time×voltage applied was 80,000 V-h. SDS-PAGE was done in polyacrylamide gels (12% T, 2.6% C) at 35 mA per gel. The spots resulting by two dimensional separation were stained by sensitive Coomassie brilliant blue G-250 stain. To ensure protein pattern

reproducibility, three technical replicates were performed.

3.3. Image analysis and statistics

Image analysis was carried out with computer software (Progenesis SameSpots, Version 2.0, Nonlinear Dynamics, Newcastle upon Tyne, UK). For each protein spot, the average spot quantity value and its variance coefficient in each group was determined. One-way analysis of variance (ANOVA) was carried out at $p < 0.05$ to assess for absolute protein changes among the different treatments. The statistically significant spots with fold ≥ 2 were cut by EXQuest Spot Cutter (Bio-Rad, CA, USA) and subjected to in-gel trypsin digestion.

3.4. Tryptic digestion

Protein bands observed in SDS-PAGE were carefully excised from silver-stained polyacrylamide gels and subjected to in-gel trypsin digestion according to Shevchenko et al.⁵⁴ with minor modifications. The supernatant containing tryptic peptides was dried by vacuum centrifugation. Prior to mass spectrometric analysis, the peptide mixtures were redissolved in 10 μ L of 5% FA (Formic Acid).

3.5. LC-ESI-CID-MS/MS (proteomic analysis)

Samples were analyzed using a split-free nano-flow liquid chromatography system (EASY-nLC II, Proxeon, Odense, Denmark) coupled to a 3D-ion trap (model AmaZon ETD, Bruker Daltonik, Germany) equipped with an online ESI nano-sprayer (the spray capillary was a fused silica capillary, 0.090 mm o.d., 0.020 mm i.d.). For all experiments a sample volume of 15 μ L was loaded by the autosampler onto a homemade 2 cm fused silica precolumn (100 μ m I.D.; 375 μ m O.D.; Reprosil C18-AQ, 5 μ m, Dr. Maisch GmbH, Ammerbuch-Entringen, Germany). Sequential elution of peptides was accomplished using a flow rate of 300 nL/min and a linear gradient from Solution A (2% acetonitrile; 0.1% formic acid) to 50% of Solution B (98% acetonitrile; 0.1% formic acid) in 40 min over the precolumn on-line with a homemade 15 cm resolving column (75 μ m I.D.; 375 μ m O.D.; Reprosil C18-AQ, 3 μ m, Dr. Maisch GmbH, Ammerbuch-Entringen, Germany). The acquisition parameters for the mass spectrometer were as follows: dry gas temperature, 220 $^{\circ}$ C; dry gas, 4.0 L/min; nebulizer gas, 10 psi; electrospray voltage, 4000 V; high-voltage end-plate offset, -200 V; capillary exit, 140 V; trap drive: 63.2; funnel 1 in, 100 V out 35 V and funnel 2 in, 12 V out 10 V; ICC target, 200 000; maximum accumulation time, 50 ms. The sample was measured with the "Enhanced Resolution Mode at 8100 m/z per second (which allows mono isotopic resolution up to four charge stages) polarity positive, scan range from m/z 300 to 1500, 5 spectra averaged, and rolling average of 1. The "Smart Decomposition" was set to "auto". Acquired CID spectra were processed in DataAnalysis 4.0, and deconvoluted spectra were further analyzed with BioTools 3.2 software and submitted to Mascot search program (in-house version 2.2, Matrix Science, London, UK). The following parameters were adopted for database searches: NCBI nr database (release date 22/09/2012; 20543454 sequences; 7050788919 residues); taxonomy=All entries; peptide and fragment mass tolerance of ± 0.3 Da; enzyme specificity trypsin with 2 missed cleavages considered; fixed modifications: carbamidomethyl (C); variable modifications: oxidation (M).

3.6. Sample preparation for metabolomic analysis

Wild type and *Ayca1* W303-1B yeast cells, grown in YPD medium up to exponential phase (OD_{600} about 0.7) were harvested and incubated in the same medium set to pH 3.00. Immediately after the pH shift (C_0), 2×10^7 cells were collected and used for metabolomic analysis. The yeast cells were resuspended in 100 μ l of ice cold ultra-pure water (18 M Ω) to lyse the cells and then the tubes were plunged alternatively into a water bath at 37 $^{\circ}$ C for 0.5 minutes and at 4 $^{\circ}$ C for 0.5 minutes. To be sure that the cells are lysed, the samples were sonicated for 10 minutes. Samples were mixed with 400 μ l of -20 $^{\circ}$ C methanol and then with 600 μ L of -20 $^{\circ}$ C chloroform. The tubes were stored at -20 $^{\circ}$ C over night. After centrifugation, we have taken the top fraction (methanol fraction) which contained metabolites.

3.7. Rapid Resolution Reversed-Phase HPLC (metabolite separation)

An Ultimate 3000 Rapid Resolution HPLC system (DIONEX, Sunnyvale, USA) was used to perform metabolite separation. The system featured a binary pump and vacuum degasser, well-plate autosampler with a six-port micro-switching valve, a thermostated column compartment. A Phenomenex Luna 3 μ m HILIC 200A (150 x 2.0 mm), protected by a guard column

HILIC 4 x 2.0mm ID (Phenomenex) was used to perform metabolite separation over a phase B to phase A gradient lasting 35 minutes. For HILIC separation, 50 mM ammonium acetate was prepared by dissolving ammonium acetate in deionized water. The aqueous ammonium acetate was mixed with acetonitrile (95:5, v/v). This was used for mobile phase 'A'. Eluent 'B' was composed of mixture of 50 mM aqueous ammonium acetate: water and acetonitrile (95:5, v/v).

Samples were loaded onto a Reprosil C18 column (2.0 mm × 150 mm, 2.5 μm — Dr Maisch, Germany) for metabolite separation. Chromatographic separations were achieved at a column temperature of 30 °C; and flow rate of 0.2 mL/min. For downstream positive ion mode (+) MS analyses, a 0–100% linear gradient of solvent A (ddH₂O, 0.1% formic acid) to B (acetonitrile, 0.1% formic acid) was employed over 30 min, returning to 100% A in 2 min and a 6-min post-time solvent A hold. Acetonitrile, formic acid, and HPLC-grade water and standards (≥98% chemical purity) were purchased from Sigma Aldrich.

3.8. Mass spectrometry: Q-TOF settings

Due to the use of linear ion counting for direct comparisons against naturally expected isotopic ratios, time-of-flight instruments are most often the best choice for molecular formula determination. Thus, mass spectrometry analysis was carried out on an electrospray hybrid quadrupole time-of flight mass spectrometer MicroTOF-Q (Bruker-Daltonik, Bremen, Germany) equipped with an ESI-ion source. Mass spectra for metabolite extracted samples were acquired both in positive and in negative ion modes. ESI capillary voltage was set at 4500 V (+) (–) ion mode. The liquid nebulizer was set to 27 psi and the nitrogen drying gas was set to a flow rate of 6 L/min. Dry gas temperature was maintained at 200 °C. Data were stored in centroid mode. Data were acquired with a stored mass range of m/z 50–1200. Calibration of the mass analyzer is essential in order to maintain a high level of mass accuracy. Instrument calibration was performed externally every day with a sodium formate solution consisting of 10 mM sodium hydroxide in 50% isopropanol: water, 0.1% formic acid. Automated internal mass scale calibration was performed through direct automated injection of the calibration solution at the beginning and at the end of each run by a 6-port divert-valve.

3.9 Untargeted metabolomics analysis

Replicates were exported as mzXML files and processed through MAVEN.⁵² Mass spectrometry chromatograms were elaborated for peak alignment, matching and comparison of parent and fragment ions, and tentative metabolite identification (within a 10 ppm mass-deviation range between observed and expected results against the imported KEGG database⁵³). MAVEN is an open-source software that could be freely downloaded from the official project websites (<http://genomics-pubs.princeton.edu/mzroll/index.php?show=download>). Scatter plot are obtained from maven.

3.10 Bioinformatics analysis

Protein sequences of all identified proteins were analyzed for the presence of tripeptide metacaspase substrates (ARR, GRR, VKKR, GGR, VLK)³⁴ by Yeast Genome Pattern Matching tool (<http://www.yeastgenome.org/cgi-bin/PATMATCH/nph-patmatch>). Genome of *S. cerevisiae* strain W303 was chosen for the analysis and translation of all *S. cerevisiae* strain W303 ORFs was chosen as a sequence database.

4. Conclusions

In this paper, we used a combination of proteomic and metabolomic analysis to identify metabolic pathways and cellular processes affected by *YCA1* deletion in *S. cerevisiae* W303-1B genetic background under physiological growth conditions. Relevant information could be retrieved when performing both proteomics and metabolomics analysis simultaneously. Our results increased the knowledge about cellular processes and proteins whose roles and functions depend on *YCA1* in yeast. The data obtained show a role of *YCA1* in the modulation of central carbon metabolism as well as amino acid and nucleotide metabolism. *YCA1* deletion appears to down-regulate glycolysis, TCA cycle and alcoholic fermentation as

compared with WT cells. *Δyca1* cells also showed a down-regulation of PPP and an accumulation of pyruvate, correlated with higher levels of certain amino acids found in these cells. Accordingly, there is a decrease in protein biosynthesis and protein transport/folding, and accumulation of various stress response proteins like Ahp1p, which possibly provides these cells with a better protection against stress.

We also identified eight proteins containing peptide sequences for which recombinant Yca1p has been shown to display endopeptidase activity³⁴. However, in no case we found evidences of accumulation of uncleaved polypeptides in *Δyca1* cells indicative of the presence of active metacaspase cleavage in WT cells. Thus, at least in our physiological growth conditions yeast metacaspase does not seem to cleave these sites.

To better understand the interactions between all proteins identified and metacaspase, we obtained a network pathway using STRING software (<http://string-db.org>) (Fig. 5). It has been already demonstrated that Yca1p participates at different steps in cell cycle dynamics¹⁸ and that has a role in proteostasis through regulation of the composition of insoluble proteins²⁰. Our combined proteome/metabolome approach added a new dimension to the non-apoptotic function of yeast metacaspase, which can specifically affect cell metabolism through as yet unknown mechanisms and possibly stress-response pathways, like HOG and cell wall integrity pathways, providing a comprehensive description of YCA1 interactome which can be used as the basis of future investigations. Thus, we think that deeper insights on specific proteins and/or metabolites will be the focus of future studies on processes/metabolisms shown in this paper to be dependent on YCA1.

5. Acknowledgements

This work has been funded by grants from project FIRB-MERIT RBNE08HWLZ, the Italian Ministry of Economy and Finance to the CNR for the Project “FaReBio di Qualità” and project BioNet –PTP - PO Regione Puglia FESR 2000-2006 to S.G.

This paper was supported by mobility award to young scientists by Italian Society of Proteomic (ItPA) to M.Z.

6. Notes and references

[#]Corresponding authors: Timperio Anna Maria University “La Tuscia” Viterbo, email: timperio@unitus.it

Zolla Lello University “La Tuscia” Viterbo, email: zolla@unitus.it

^a CNR, Istituto di Biomembrane e Bioenergetica, Via Amendola 165/a, 70126 Bari, Italy;

^b Department of Ecological and Biological Sciences, University of Tuscia, Largo dell'Università, snc, 01100 Viterbo, Italy.

*The authors contributed equally to this work

[‡]SUNY Upstate Medical University, Syracuse NY, USA.

1. L. Aravind and E. V. Koonin, *Proteins*, 2002, **46**, 355-367.
2. D. W. Nicholson and N. A. Thornberry, *Trends in biochemical sciences*, 1997, **22**, 299-306.
3. W. C. Earnshaw, L. M. Martins and S. H. Kaufmann, *Annual review of biochemistry*, 1999, **68**, 383-424.
4. G. S. Salvesen and V. M. Dixit, *Cell*, 1997, **91**, 443-446.
5. D. Hanahan and R. A. Weinberg, *Cell*, 2000, **100**, 57-70.
6. S. Fulda, *Int J Cancer*, 2009, **124**, 511-515.
7. B. Fadeel, S. Orrenius and B. Zhivotovsky, *Biochemical and biophysical research communications*, 1999, **266**, 699-717.
8. N. A. Thornberry and Y. Lazebnik, *Science*, 1998, **281**, 1312-1316.
9. C. Pop and G. S. Salvesen, *The Journal of biological chemistry*, 2009, **284**, 21777-21781.
10. A. G. Uren, K. O'Rourke, L. A. Aravind, M. T. Pisabarro, S. Seshagiri, E. V. Koonin and V. M. Dixit, *Mol Cell*, 2000, **6**, 961-967.
11. L. Tsiatsiani, F. Van Breusegem, P. Gallois, A. Zavalov, E. Lam and P. V. Bozhkov, *Cell death and differentiation*, 2011, **18**, 1279-1288.
12. D. Carmona-Gutierrez, T. Eisenberg, S. Buttner, C. Meisinger, G. Kroemer and F. Madeo, *Cell death and differentiation*, 2010, **17**, 763-773.
13. L. Portt, G. Norman, C. Clapp, M. Greenwood and M. T. Greenwood, *Biochimica et biophysica acta*, 2011, **1813**, 238-259.
14. M. Zdravleic, N. Guaragnella, L. Antonacci, E. Marra and S. Giannattasio, *ScientificWorldJournal*, 2012, **2012**, 912147.
15. F. Madeo, E. Herker, C. Maldener, S. Wissing, S. Lachelt, M. Herlan, M. Fehr, K. Lauber, S. J. Sigrist, S. Wesselborg and K. U. Frohlich, *Mol Cell*, 2002, **9**, 911-917.
16. F. Madeo, D. Carmona-Gutierrez, J. Ring, S. Buttner, T. Eisenberg and G. Kroemer, *Biochemical and biophysical research communications*, 2009, **382**, 227-231.
17. N. Guaragnella, C. Pereira, M. J. Sousa, L. Antonacci, S. Passarella, M. Corte-Real, E. Marra and S. Giannattasio, *FEBS letters*, 2006, **580**, 6880-6884.
18. R. E. Lee, L. G. Puente, M. Kaern and L. A. Megeney, *PLoS one*, 2008, **3**, e2956.
19. R. E. Lee, S. Brunette, L. G. Puente and L. A. Megeney, *Proceedings of the National Academy of Sciences of the United States of America*, 2010, **107**, 13348-13353.
20. A. Shrestha, L. G. Puente, S. Brunette and L. A. Megeney, *Journal of proteomics*, 2013, **81**, 24-30.
21. S. M. Hill, X. Hao, B. Liu and T. Nystrom, *Science*, 2014, **344**, 1389-1392.
22. M. A. Khan, P. B. Chock and E. R. Stadtman, *Proceedings of the National Academy of Sciences of the United States of America*, 2005, **102**, 17326-17331.

23. S. Lefevre, D. Sliwa, F. Auchere, C. Brossas, C. Ruckenstuhl, N. Boggetto, E. Lesuisse, F. Madeo, J. M. Camadro and R. Santos, *FEBS letters*, 2012, **586**, 143-148.
24. M. P. Washburn, D. Wolters and J. R. Yates, 3rd, *Nature biotechnology*, 2001, **19**, 242-247.
25. A. Silva, B. Almeida, B. Sampaio-Marques, M. I. Reis, S. Ohlmeier, F. Rodrigues, A. Vale and P. Ludovico, *Biochimica et biophysica acta*, 2011, **1813**, 2044-2049.
26. J. G. Meyer, Komives, E.A., *J. Am. Soc. Mass Spectrom.*, 2012, **23**, 1390-1399.
27. H. Hahne, F. Pachi, B. Ruprecht, S. K. Maier, S. Klaeger, D. Helm, G. Medard, M. Wilm, S. Lemeer and B. Kuster, *Nat Meth*, 2013, **10**, 989-991.
28. A.S. Hebert, A.L. Richards, D.J. Bailey, A. Ulbrich, E.E. Coughlin, M.S. Westphall, J.J. Coon. *Mol Cell Proteomics*. 2014, **13**, 339-47.
29. V. Carmelo, P. Bogaerts and I. Sa-Correia, *Arch Microbiol*, 1996, **166**, 315-320.
30. A. P. Gasch and M. Werner-Washburne, *Functional & integrative genomics*, 2002, **2**, 181-192.
31. M. F. Clasquin, E. Melamud and J. D. Rabinowitz, *Current protocols in bioinformatics / editorial board, Andreas D. Baxeavanis ... [et al.]*, 2012, **Chapter 14**, Unit14 11.
32. F. Rolland, J. Winderickx and J. M. Thevelein, *FEMS Yeast Res*, 2002, **2**, 183-201.
33. R. Diaz-Ruiz, M. Rigoulet and A. Devin, *Biochimica et biophysica acta*, 2011, **1807**, 568-576.
34. N. Watanabe and E. Lam, *The Journal of biological chemistry*, 2005, **280**, 14691-14699.
35. J. R. Dickinson, L. E. Salgado and M. J. Hewlins, *The Journal of biological chemistry*, 2003, **278**, 8028-8034.
36. E. P. Wehner, E. Rao and M. Brendel, *Molecular & general genetics : MGG*, 1993, **237**, 351-358.
37. L. A. Hazelwood, J. M. Daran, A. J. van Maris, J. T. Pronk and J. R. Dickinson, *Applied and environmental microbiology*, 2008, **74**, 2259-2266.
38. H. Saito and F. Posas, *Genetics*, 2012, **192**, 289-318
39. R. D. Silva, R. Sotoca, B. Johansson, P. Ludovico, F. Sansonetty, M. T. Silva, J. M. Peinado and M. Corte-Real, *Mol Microbiol*, 2005, **58**, 824-834.
40. H. Robichon-Szulmajster, Y. Surdin and R. K. Mortimer, *Genetics*, 1966, **53**, 609-619.
41. Y. Hernando, A. T. Carter, A. Parr, B. Hove-Jensen and M. Schweizer, *The Journal of biological chemistry*, 1999, **274**, 12480-12487.
42. R. George, Beddoe, T., Landl, K., Lithgow, T., *Proc. Natl. Acad. Sci. USA*, 1997, **95**, 2296-2301.
43. J. R. Warner, J. Vilardeell and J. H. Sohn, *Cold Spring Harbor symposia on quantitative biology*, 2001, **66**, 567-574.
44. M. Rinnerthaler, S. Jarolim, G. Heeren, E. Palle, S. Perju, H. Klinger, E. Bogengruber, F. Madeo, R. J. Braun, L. Breitenbach-Koller, M. Breitenbach and P. Laun, *Biochimica et biophysica acta*, 2006, **1757**, 631-638.
45. N. Guaragnella, A. Bobba, S. Passarella, E. Marra and S. Giannattasio, *FEBS letters*, 2010, **584**, 224-228.
46. D. Wilkinson and M. Ramsdale, *Biochem Soc Trans*, 2011, **39**, 1502-1508.
47. F. Kepes and R. Schekman, *The Journal of biological chemistry*, 1988, **263**, 9155-9161.
48. J. M. Francois, C. Formosa, M. Schiavone, F. Pillet, H. Martin-Yken and E. Dague, *Current genetics*, 2013, **59**, 187-196.
49. P. J. Plant, M. F. Manolson, S. Grinstein and N. Demaurex, *The Journal of biological chemistry*, 1999, **274**, 37270-37279.
50. L. Antonacci, N. Guaragnella, M. Zdravlevic, S. Passarella, E. Marra and S. Giannattasio, *Current Pharmaceutical Biotechnology*, 2012, **in press**.
51. R. Martin, J. J. Berlanga and C. de Haro, *Journal of cell science*, 2013, **126**, 3010-3020.
52. E. Oxelmark, A. Marchini, I. Malanchi, F. Magherini, L. Jaquet, M. A. Hajibagheri, K. J. Blight, J. C. Jauniaux and M. Tommasino, *Molecular and cellular biology*, 2000, **20**, 7784-7797.
53. J. M. Kim, H. Yoshikawa and K. Shirahige, *Genes to cells : devoted to molecular & cellular mechanisms*, 2001, **6**, 507-517.
54. A. Shevchenko, M. Wilm, O. Vorm, M. Mann, *Anal Biochem*. 1996, **68**, 850-858.

Table 1. Putative metacaspase-specific tripeptide cleavage sites in proteins showing changes in abundance between WT and $\Delta yca1$ cells . All the proteins whose amount was changed between WT and $\Delta yca1$ cells were analyzed by Yeast Genome Pattern Matching (<http://www.yeastgenome.org/cgi-bin/PATMATCH/nph-patmatch>) for the presence of one or more peptide sequences for which recombinant Yca1p has been reported to display endopeptidase activity (Watanabe & Lam, 2005). Sequence pattern, together with its start and stop position in the protein sequence are reported.

Sequence name (Protein ID)	Hit number	Match pattern	Match start position	Match stop position
YGR119C (Nup57p)	1	VLK	293	295
YOL086C (Adh1p)	1	VLK	232	234
YDL055C (Psa1p)	1	VLK	96	98
YLR301W (Hri1p)	1	VLK	157	159
YHR203C (Rps4bp)	1	GGR	185	187
YJR009C (Tdh2p)	1	GGR	196	198
YNL178W (Rps3p)	1	GRR	63	65
YHL011C (Prs3p)	1	ARR	85	87

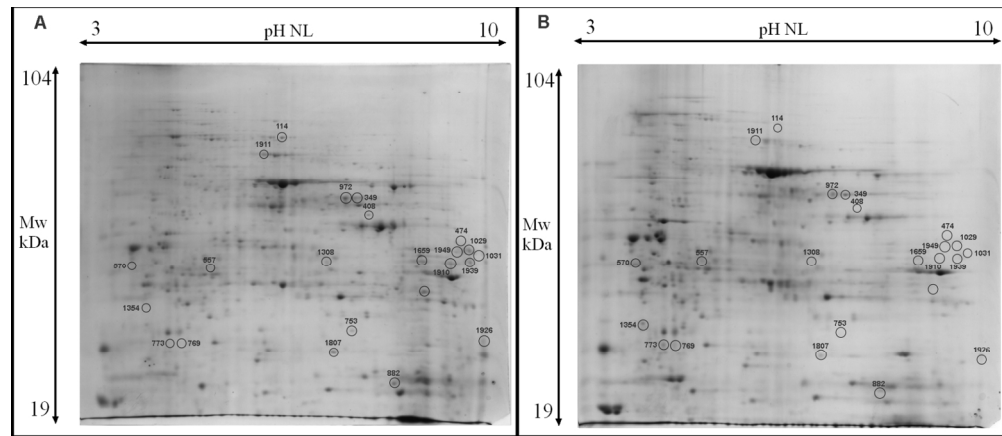


Figure 1. Representative 2-DE Coomassie-stained gels of total protein extract of W303-1B wild type and $\Delta yca1$ *S. cerevisiae* cells. Statistically significant differential spots (p value < 0.05 and fold change > 2) for WT (panel A) vs $\Delta yca1$ (panel B) analysis are reported in both panels. Molecular weight (MW) and pI range of the first dimension strips (3-10 NL) are indicated on the appropriate axis. Numbers identify proteins with altered expression between the two gels, given as in Table 1. All experiments were performed in triplicate. 229x99mm (200 x 200 DPI)

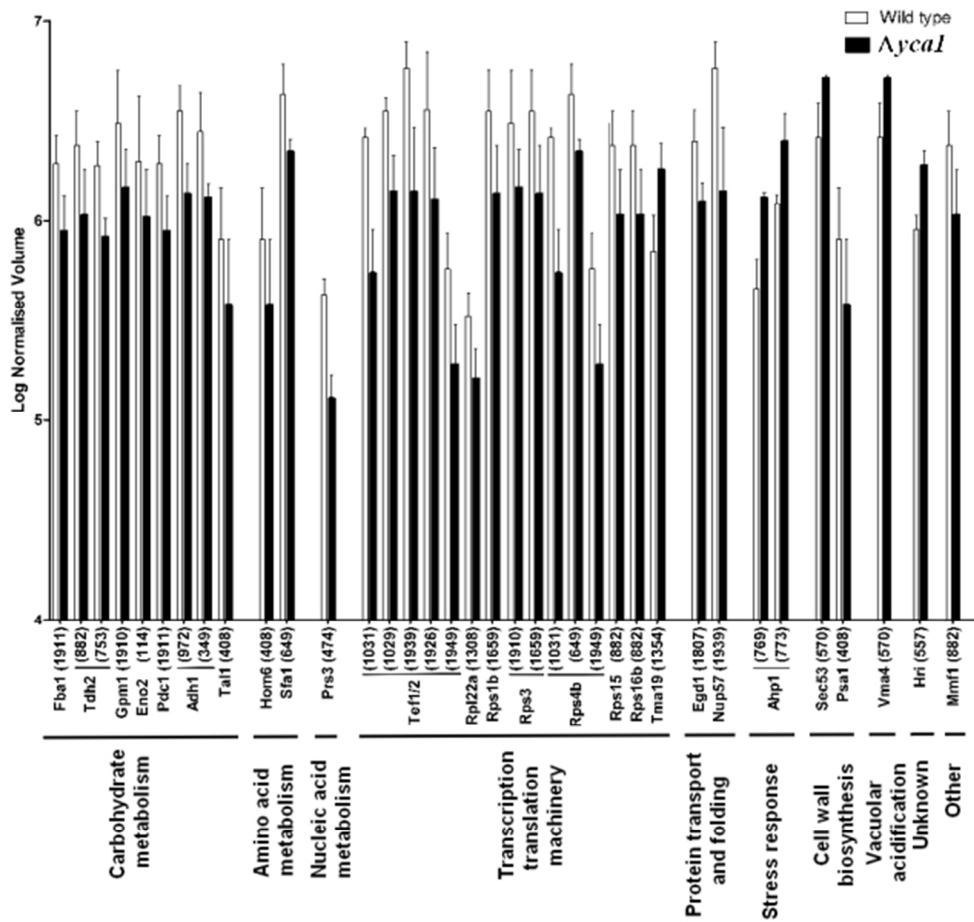


Figure 2. Relative protein expression changes of $\Delta yca1$ with respect to the wild type cells. Black bars ($\Delta yca1$) and white bars (WT) represent the mean of normalized volume of single spot from 3 different replicates (in logarithmic scale) with correspondent standard deviation (SD), calculated by Progenesis SameSpots software Version 2.0, (Nonlinear Dynamics 230x215mm (72 x 72 DPI))

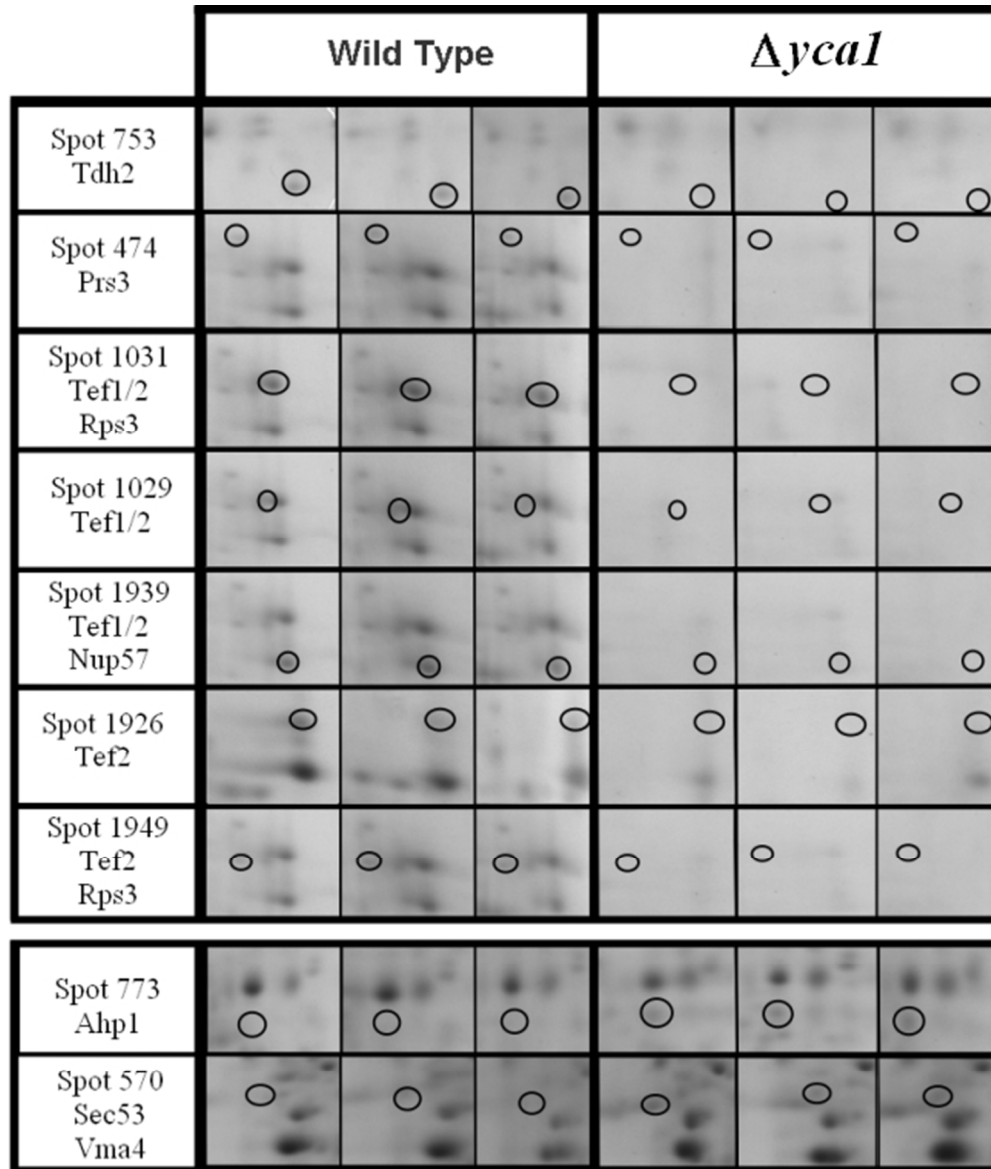


Figure 3. Magnified regions of triplicate 2-D gel images of protein spots detected exclusively in wild type or $\Delta yca1$ cells. The number and the corresponding protein(s) are indicated for every spot. Spots 753, 474, 1031, 1029, 1939, 1926 and 1949 were detected only in wild type cells (corresponding to Tdh2, Prs3, Tef 1/2, Rps3 and Nup57), whereas spots 773 and 570 were present only in $\Delta yca1$ cells (corresponding to Ahp1, Vma and Sec54).

230x269mm (72 x 72 DPI)

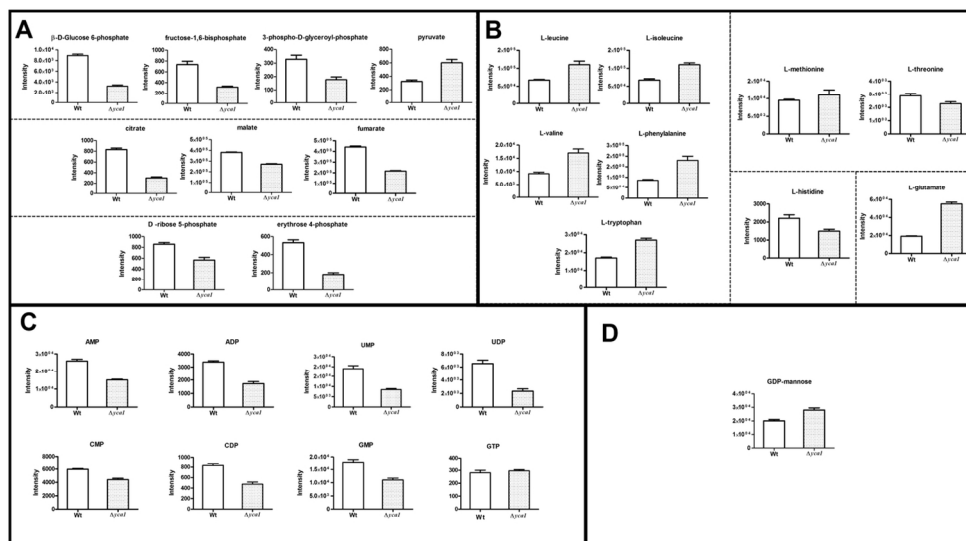


Figure 4. Absolute metabolomics quantification. Arbitrary ion counts of metabolites from carbohydrate metabolism (panel A) (glycolysis, citric acid cycle and pentose phosphate pathway), amino acid metabolism (panel B), nucleic acid metabolism (panel C) and cell wall biosynthesis (panel D) in W303-1B *S. cerevisiae* wild type (white bars) and $\Delta yca1$ cells (dotted bars). Data are presented as mean \pm SD. 127x70mm (300 x 300 DPI)

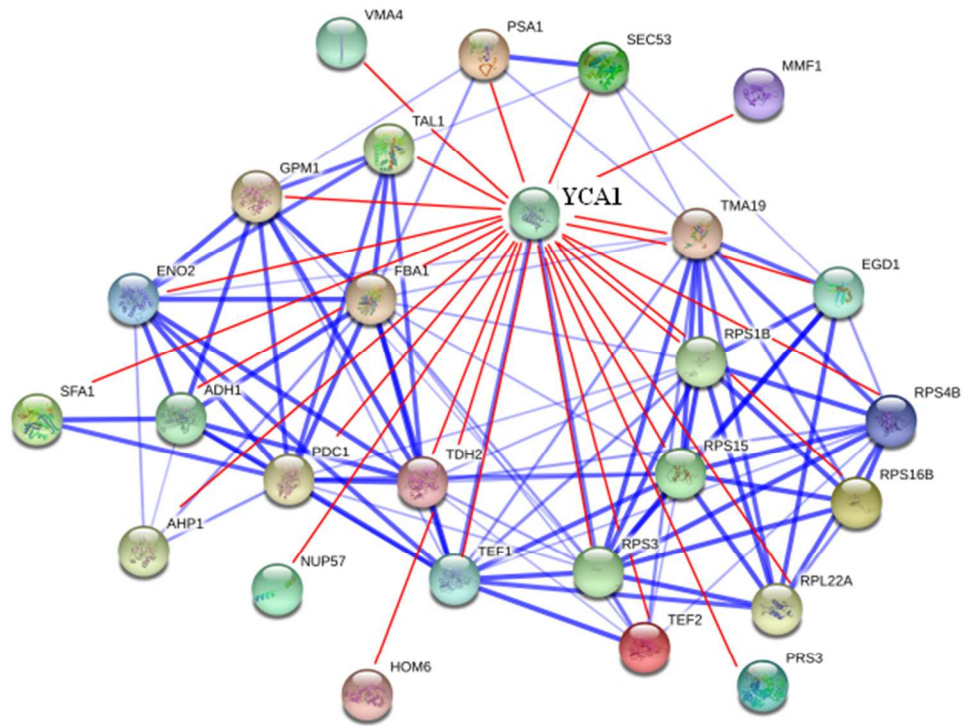


Figure 5. STRING Analysis (<http://string-db.org>). STRING Analysis of the proteins down/up-regulated by metacaspase. Red and blue double lines represent known protein interactions of YCA1, red single lines are new YCA1 interactors found and involved in cell metabolism and stress-response pathways. 230x184mm (72 x 72 DPI)